Article

Isolation, X-ray Crystal Structure and Theoretical Calculations of the New Compound 8-Epicordatin and Identification of others Terpenes and Steroids from the Bark and Leaves of *Croton palanostigma* Klotzsch

Davi S. B. Brasil,[a,b] Adolfo H. Müller,[*,a,c] Gisele M. S. P. Guilhon,[a] Cláudio N. Alves,[a] Gabriel Peris,[d] Rosa Llusar[d] and Vicent Moliner[d]*

[a]*Instituto de Ciências Exatas e Naturais, Universidade Federal do Pará, Av. Augusto Corrêa, 01, 66075-900 Belém-PA, Brazil*

[b]*Faculdade de Engenharia Química, Instituto de Tecnologia, Universidade Federal do Pará, Av. Augusto Corrêa, 01, 66075-900 Belém-PA, Brazil*

[c]*Centro Universitário do Estado do Pará, Av Nazaré, 630, 66035-170 Belém-PA, Brazil*

[d]*Departament de Química Física i Analítica, Universitat Jaume I, 12071, Castellón, Spain*

Estudos fitoquímicos com as cascas do caule e com as folhas de *Croton palanostigma* Klotzsch (Euphorbiaceae) levaram ao isolamento do novo diterpeno clerodânico 8-epicordatina (**2**), além de éster metílico do ácido 12-oxohardwickiico (**3**), aparisthmano, cordatina (**1**), ácido *ent*-trachiloban-18-óico, óxido de *ent*-13-epimanoila, óxido de *ent*-3-oxo-13-epimanoila, óxido de *ent*-3β-hidroxi-13-epimanoila, sitosterol, estigmasterol, estigmastan-3-ona, 6β-hidroxiestigmast-4-en-3-ona, 6β-hidroxiestigmasta-4,22-dien-3-ona, estigmast-4-en-3-ona, estigmasta-4,22-dien-3-ona, ácido 3-*O*-acetilaleuritolico, 11α-hidroxiurs-12-en-3-ona, α-amirenona, 24-metilenocicloartenona e lupenona. Estas substâncias foram isoladas através de procedimentos fitoquímicos usuais e suas estruturas foram deduzidas por estudos espectroscópicos, incluindo experimentos em 2D. Adicionalmente, a estrutura cristalina de 8-epicordatina (**2**) foi determinada por difração de raios-X. Cálculos teóricos de RMN ao nível B3PW91/DGDZVP foram usados para confirmação dos assinalamentos dos deslocamentos químicos dos hidrogênios H-7α e H-7β de 8-epicordatina.

Phytochemical studies of the bark and leaves of *Croton palanostigma* Klotzsch (Euphorbiaceae) led to the isolation of a new clerodane diterpene, 8-epicordatin (**2**), in addition to 12-oxohardwickiic acid methyl ester (**3**), aparisthman, cordatin (**1**), *ent*-trachyloban-18-oic acid, *ent*-13-epimanoyl oxide, *ent*-3-oxo-13-epimanoyl oxide, *ent*-3β-hydroxy-13-epimanoyl oxide, sitosterol, stigmasterol, stigmastan-3-one, 6β-hydroxystigmast-4-en-3-one, 6β-hydroxystigmasta-4,22-dien-3-one, stigmast-4-en-3-one, stigmasta-4,22-dien-3-one, 3-*O*-acetylaleuritolic acid, 11α-hydroxyurs-12-en-3-one, α-amyrenone, 24-methylenecycloartenone and lupenone. These compounds were isolated using typical phytochemical procedures and the structures were deduced from spectroscopic studies, including 2D NMR experiments. In addition, the crystalline structure of 8-epicordatin (**2**) was determined by X-ray diffraction. NMR theoretical calculations at the B3PW91/DGDZVP level were used to confirm the assignment of the chemical shifts of the H-7α and H-7β hydrogens of 8-epicordatin.

Keywords: *Croton palanostigma* Klotzsch, terpenes, steroids, NMR DFT calculations, X-ray crystallography

Introduction

Croton palanostigma Klotzsch (Euphorbiaceae) is a medium-sized tree native to the Northern Brazilian coastal region. Phytochemical studies of the bark of *C. palanostigma* under the erroneous identification of *Aparisthmium cordatum*[1] yielded two furan diterpenes with a clerodane skeleton, namely, aparisthman[2] and cordatin (**1**).[3] These compounds showed anti-ulcer activity similar to that of cimetidine (Tagamet®), a compound used for the

*e-mail: muller@ufpa.br, muller@cesupa.br

treatment of peptic ulcers.[4,5] This species, together with various *Croton* spp., is known to produce a red viscous sap called dragon's blood. The sap of *C. palanostigma* is reported to have various pharmacological and physiological actions.[6] Phytochemical studies of dragon's blood obtained from *Croton* spp. led to the isolation of the alkaloid taspine,[7] the dihydrobenzofuran lignans 3′,4-*O*-dimethylcedrusin[8] and 4-*O*-methylcedrusin,[9] and proanthocyanidins.[10]

The principal mechanism of the anti-ulcerogenic effect of cordatin (**1**) remains unknown. It seems to be related to an anti-secretory property, but the involvement of a mucosal defensive mechanism should not be ignored.[5] Other anti-ulcerogenic drugs, such as the proton pump inhibitors omeprazole, lansoprazole and pantoprazole, exist as pro-drugs that need activation for interaction with gastric H⁺,K⁺-ATPase.[11] Protonation of these compounds results in extensive molecular rearrangement followed by the formation of a positively charged sulfenamide species that has a low permeability coefficient across membranes and reacts covalently with free sulfhydryl group(s) on the extracellular surface of H⁺,K⁺-ATPase.[12] The sulfonamide forms a disulfide that covalently modifies the enzyme's extracellular domain and inhibits it with a stoichiometry of ~2 molecules of drug per subunit of H⁺,K⁺-ATPase.[11]

In the present work, a new phytochemical study of *C. palanostigma* was undertaken. The dichloromethane extract of the bark resulted in the new compound 8-epicordatin (**2**) (Figure 1). The hexane extract of the bark yielded 12-oxohardwickiic acid methyl ester (**3**), together with other six diterpenoids, seven steroids and one triterpenoid. The hexane extract of the leaves yielded four triterpenoids. This study demonstrates the use of theoretical calculations in determining geometric parameters, chemical shifts and NMR coupling constants. The molecular electrostatic potential (MEP) was also calculated to define the most probable sites of interaction of **1** and **2** with H⁺ ions in gastric fluid.
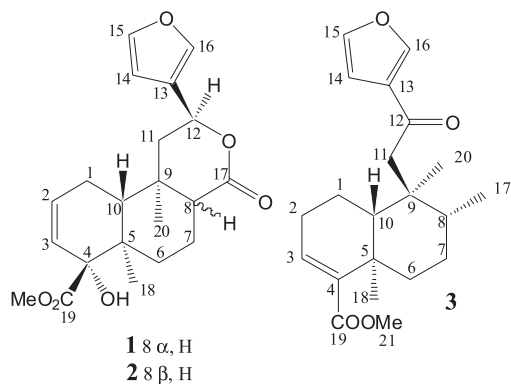
Results and Discussion

The structures of the isolated compounds were deduced mainly from ¹H and ¹³C NMR spectroscopic data at 300 and 75.4 MHz, respectively, with the aid of ¹H, ¹H-COSY, ¹³C,¹H-COSY-¹*J* (CH) and ¹³C, ¹H-COSY-²;³*J* (CH) spectra. DEPT pulse sequences were used to determine the hydrogenation pattern of the carbons.

12-Oxohardwickiic acid methyl ester (**3**) was isolated as an oil. Its molecular formula is $C_{21}H_{28}O_4$ (EIMS). Its IR spectrum is consistent with the presence of two conjugated carbonyl groups corresponding to peaks at 1668 (ketone adjacent to a furan ring) and 1714 cm⁻¹ (ester adjacent to a double bond) and a furan ring (3135, 1509 and 872 cm⁻¹).[13] Table 1 shows the ¹H and ¹³C NMR spectroscopic data for **3**; these data are in complete agreement with those reported in the literature for **3,** which was obtained by oxidation of 12-hydroxyhardwickiic acid methyl ester, isolated from a hexane extract of the roots of *Croton sonderianus*.[14] This compound (**3**) was isolated for the first time as a natural product from *Croton polyandrous*.[15]

The new natural product 8-epicordatin (**2**) was isolated as crystals. Its IR spectrum is consistent with the presence of an O–H group (3540 cm⁻¹), two carbonyl groups corresponding to peaks at 1704 (δ-lactone) and 1733 cm⁻¹ (methyl ester) and a furan ring (3100, 1503 and 873 cm⁻¹).[13] Its molecular formula is $C_{21}H_{26}O_6$ (HRMS). This compound was identified by comparison of its NMR data (Table 1) with those reported in the literature for cordatin (**1**)[3] crotobrasilin A[16] and epi-cordatin.[17] In addition, the NOESY data are similar to those reported in the literature used to propose the relative configurations at asymmetric centers for crotobrasilin A[16] (Figure 2). Therefore, the new natural product 8-epicordatin (**2**) is the non-acetylated form of crotobrasilin A.[16] Finally, the structure of 8-epicordatin (**2**) was also confirmed by X-ray diffraction. The ORTEP representation for the molecular labeling in the X-ray structure of **2** is shown in Figure 3. The most relevant X-ray
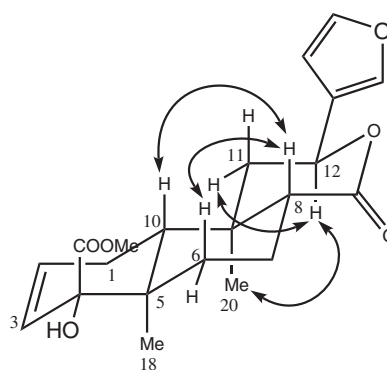

Figure 1. Structures of **1**, **2** and **3**.

Figure 2. Significant NOESY correlations of **2**.

Table 1. NMR spectroscopic data[a] (300 and 75.4 MHz, CDCl$_3$) for cordatin (**1**), 8-epicordatin (**2**) and 12-oxohardwickiic acid methyl ester (**3**)

Position	Cordatin (**1**)		8-Epicordatin (**2**)		12-Oxohardwickiic acid methyl ester (**3**)	
	δ_C, mult.	δ_H (*J* in Hz)	δ_C, mult.	δ_H (*J* in Hz)	δ_C, mult.	δ_H (*J* in Hz)
1	23.1, CH$_2$	2.02, m	22.9, CH$_2$	2.10, m	18.9, CH$_2$	α, 1.52, ddd (1.3, 7.5, 13.5) β, 1.76, m
2	130.0, CH	5.93, ddd (2.7, 4.6, 10.1)	130.0, CH	5.95, ddd (2.9, 4.6, 10.0)	27.0, CH$_2$	α, 2.15, m β, 2.07, ddd (3.3, 7.5, 11.4)
3	128.5, CH	5.31, dt (2.3, 10.1)	128.7, CH	5.36, ddd (1.8, 2.5, 10.0)	137.3, CH	6.56, dd (3.3, 4.5)
4	80.7, $_q$C		81.2, $_q$C		141.9, $_q$C	
5	40.6, $_q$C		40.5, $_q$C		37.9, $_q$C	
6	28.4, CH$_2$	α, 1.54, dt (3.6, 13.4) β, 1.36, m	33.2, CH$_2$	α, 1.86, dt (2.7, 13.3) β, 0.91, td (3.0, 13.3)	35.3, CH$_2$	α, 2.23, dt (3.0, 12.7) β, 1.12, m
7	17.7, CH$_2$	α, 1.78, m β, 2.10, dq (3.6, 15.2)	18.1, CH$_2$	a, 1.60, m b, 2.10, m	27.4, CH$_2$	1.40, m
8	44.9, CH	2.48, dd (1.9, 3.6)	51.4, CH	2.07, m	37.3, CH	1.86, m
9	35.3, $_q$C		36.4, $_q$C		42.4, $_q$C	
10	44.7, CH	2.29, dd (5.6, 10.4)	44.7, CH	2.33, dd (5.2, 11.0)	47.1, CH	1.70, dd (1.3, 13.5)
11	48.9, CH$_2$	α, 2.00, dd (1.8, 14.1) β, 1.78, m	44.4, CH$_2$	α, 2.29, dd (5.4, 13.6) β, 1.67, dd (11.7, 13.6)	47.6, CH$_2$	a, 2.70, d (14.8) b, 2.77, d (14.8)
12	69.8, CH	5.24 br, d (11.0)	71.9, CH	5.48, dd (5.4, 11.7)	194.9, $_q$C	
13	123.9, $_q$C		125.8, $_q$C		129.6, $_q$C	
14	108.5, CH	6.42, dd (0.9, 1.9)	108.5, CH	6.41, dd (0.9, 1.9)	108.9, CH	6.73, dd (0.8, 1.9)
15	143.6, CH	7.41, t (1.9)	143.7, CH	7.41, t (1.9)	144.1, CH	7.41, dd (1.4, 1.9)
16	139.6, CH	7.47 br, s	139.3, CH	7.44, m	146.7, CH	7.99, dd (0.8, 1.4)
17	173.8, $_q$C		171.9, $_q$C		16.6, CH$_3$	0.90, d (6.8)
18	14.8, CH$_3$	1.10, s	15.2, CH$_3$	1.12, s	20.6, CH$_3$	1.26, s
19	175.9, $_q$C		175.5, $_q$C		167.7, $_q$C	
20	24.4, CH$_3$	1.32, s	15.4, CH$_3$	1.17, s	17.6, CH$_3$	0.84, s
21	53.4, CH$_3$	3.78, s	53.2, CH$_3$	3.81, s	51.0, CH$_3$	3.66, s

[a]^{1}H NMR referenced to CHCl$_3$ at δ 7.26 ppm; ^{1}H, ^{1}H-COSY spectra were used to determine spin-spin interactions.^{13}C NMR referenced to CHCl$_3$ at δ 77.00 ppm. All assignments were confirmed by ^{1}H, ^{1}H-COSY ^{13}C, ^{1}H-COSY-$^1 J_{CH}$ and ^{13}C, ^{1}H-COSY-$^{2;3} J_{CH}$ experiments.
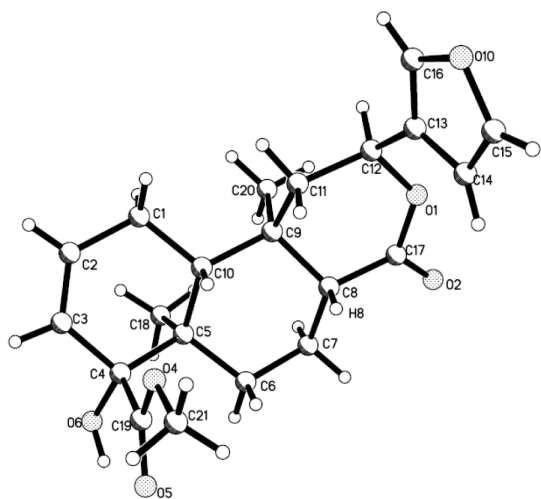
Figure 3. ORTEP representation of **2**.

and theoretical structural parameters for **2** are shown in Tables 2 and 3; complete data for the X-ray structure are shown in the supplementary material.

The configurations of the asymmetrical centers of aparisthman and cordatin (**1**) were determined by comparison of their NMR spectroscopic data with those obtained for authentic samples. Detailed NMR data for **1** are presented in Table 1.

The known compounds were identified by comparison of their spectroscopic data with those reported in the literature. The ^{13}C NMR spectral signals of *ent*-trachyloban-18-oic acid at δ 16.2 (Me-19) and 14.9 (Me-20) excluded the possible epimer *ent*-trachyloban-19-oic acid[18] [δ 28.8 (Me-18) and 12.4 (Me-20)]. Furthermore, the configuration of *ent*-8α,13S to *ent*-3-oxo-13-epimanoyl oxide was confirmed by comparison of its optical rotation,

Table 2. Crystallographic data for **2**

Empirical formula	$C_{21}H_{26}O_6$
Molecular weight	374.42
Temperature	273(2) K
Wavelength	0.71073 Å
Crystal system	Tetragonal
Space group	P4(1)2(1)2
Unit cell dimensions	$a = 11.9617(5)$ Å, $\alpha = 90°$
	$b = 11.9617(5)$ Å, $\beta = 90°$
	$c = 26.1728(15)$ Å, $\gamma = 90°$
Volume	3744.9(3) Å^3
Z	8
Density (calculated)	1.328 g/m^3
Absorption coefficient	0.097 mm^{-1}
F(000)	1600
Crystal size	0.50×0.36×0.29 mm^3
θ range for data collection	1.87-26.37°
Index ranges	$-10 \leq h \leq 10$, $0 \leq k \leq 14$, $0 \leq l \leq 32$
Reflections collected	3832
Independent reflections	3832 [R(int)=0.0000]
Completeness to θ = 26.37°	100.0%
Absorption correction	Semi-empirical from equivalents
Max. and min. transmission	0.9725 and 0.9532
Refinement method	Full-matrix least-squares on F^2
Data/restraints/parameters	3832/0/249
Goodness-of-fit of F^2	1.015
Final R indices [I > 2sigma(I)]	R1 = 0.0576, wR2 = 0.1489
R indices (all data)	R1 = 0.0915, wR2 = 0.1775
Extinction coefficient	0.0063(13)
Largest diff. peak and hole	0.243 and −0.179 e Å^{-3}

$[\alpha]_D^{25}$ −50.9° (CHCl$_3$, *c* 0.11) and spectroscopic data to those reported in the literature.[19] The same configuration was proposed for *ent*-13-epimanoyl oxide and *ent*-3β-hydroxy-13-epimanoyl oxide.

The atomic distances, angles and torsion angles for both X-ray and B3LYP/6-31G(*d,p*) optimized structures of **2** presented in Table 3 are common for this type of compound. The hydroxyl group O6-H is involved in an intramolecular hydrogen bond with O5 at 2.128 Å (1.941 Å in calculations).

The crystallographic parameters for **2** were compared with data from the literature for **1**,[1,3] revealing similar structural parameters in the case of a *trans* relationship between the methyl group (C-20) attached to C-9 and the hydrogen borne by C-10, and the same type of relationship between the methyl group (C-18) attached to C-5 and the

carbonyl carbon (C-19) linked to C-4. The *cis* relationship existing between the hydrogen on C-8 and the methyl group (C-20) located at C-9 in **1**[1,3] is not present in **2**. In this case, a *trans* relationship is observed. These results demonstrate that **2** has a *trans*-clerodane skeleton with a chair conformation for ring B and half-chair conformations for rings A and C due to the location of the double bond between C-2 and C-3 and the ester group at C-17.

Table 3. Experimental and theoretical structural parameters for 2

Structural parameters	Experimental[a]	B3LYP/6-31G(*d,p*)
Bond distance (Å)		
C4–C19	1.533(4)	1.553
C19–O5	1.205(3)	1.218
C19–O4	1.317(4)	1.338
O4–C21	1.437(3)	1.443
C4–O6	1.432(4)	1.421
C9–C20	1.536(4)	1.546
C5–C18	1.549(4)	1.548
C17–O2	1.214(5)	1.208
C12–C13	1.494(6)	1.498
Bond angle (°)		
C4–C19–O5	123.6(3)	121.7
C4–C19–O4	113.4(2)	115.2
O5–C19–O4	123.0(3)	123.1
C19–O4–C21	117.5(2)	115.5
C3–C4–O6	106.5(3)	108.1
C10–C9–C20	114.2(2)	113.9
C8–C17–O2	123.5(6)	123.5
C20–C9–C11	109.8(3)	109.1
C11–C12–C13	112.5(3)	112.8
C4–C5–C18	107.1(3)	106.3
O1–C12–C13	106.6(3)	107.3
Dihedral angles (°)		
C5–C4–C19–O4	75.1	74.7
C5–C4–C19–O5	−105.4	−106.2
C4–C19–O4–C21	178.8	179.5
C6–C7–C8–C17	171.0	168.5
O5–C19–O4–C21	−0.7	0.4
C20–C9–C8–C17	56.0	60.5
C20–C9–C11–C12	−60.5	−58.7
C9–C11–C12–C13	−154.9	−165.9
C11–C12–C13–C16	−88.2	−111.1
C11–C12–C13–C14	86.8	67.1
O1–C12–C13–C14	−40.1	−58.9
O1–C12–C13–C16	144.9	122.9

[a]Estimated standard deviation in parentheses.

The ^{1}H and ^{13}C NMR spectra were calculated for **2** and TMS (internal standard) (shielding constants of 32.1843 to ^{1}H and 186.3296 to ^{13}C). Calculated and experimental ^{1}H and ^{13}C NMR chemical shifts, as well as theoretical, predicted and experimental results for the coupling constants [^nJ (H-H)] of **2** are presented in the supplementary material. The most relevant statistical parameters are presented in Table 4. Figure 4 shows the correlation between calculated and experimental ^{1}H chemical shifts (A), ^{13}C chemical shifts (B) and coupling constants (C). Statistical analysis revealed good correlation for the model of ^{1}H and ^{13}C chemical shifts (R^2 = 99.41%, F = 2703.85, s = 0.19, Q^2 = 99.26% for ^{1}H and R^2 = 99.89%, F = 18054.82, s = 1.84, Q^2 = 99.86% for ^{13}C) (Figure 4 A and B). Calculations for the coupling constant yielded slightly worse results compared to those for the chemical shifts (Figure 4 C) (R^2 = 94.68%, F = 289.42, s = 1.22, Q^2 = 92.80%), but they are considered satisfactory. These results confirm the relevance of the theoretical data used to confirm chemical shifts for the hydrogens H-7α (1.60 experimental and 1.55 predicted) and H-7β (2.10 experimental and 2.32 predicted) because the NMR experiments performed did not allow this definition.

In Figure 4B, we can see that the general correlation to statistical analysis of ^{13}C NMR parameters is satisfactory, because all signals originating from different functional groups fall into their own distinctive regions. Thus, the overall reliability of this calculation is borne out. However some signals appear in reverse order than they would in the experimental spectrum. We note that these inversions do occur, nevertheless, only for closely spaced points, hence presumably originating from nuclei in the same functional group. The order is correct for 17 (out of 21) ^{13}C NMR signals, but two pairs are interchanged with respect to the experimental ordering: C-2, C-3 (theoretical = 137.6 and 139.5 ppm; experimental = 130.0 and 128.7 ppm, respectively) and C-10, C-11(theoretical = 50.1 and 51.3 ppm; experimental = 44.7 and 44.4 ppm, respectively).

Despite the significant results in the statistical analysis, the individual differences between experimental and theoretical ^{13}C NMR data are considerably high. For example, there are chemical shifts of some sp^2 carbons

Table 4. Correlation and fitting parameters for calculated NMR properties of **2**[a]

	A	b	R^2	F	s	Q^2
δ (^{1}H)	−0.17	1.03	99.41%	2703.85	0.19	99.26%
δ (^{13}C)	3.91	1.03	99.89%	18054.82	1.84	99.86%
^nJ(H–H)	0.05	1.08	94.68%	289.42	1.22	92.80%

[a]Linear fitting parameters refer to $\delta_{calcd} = a + b\delta_{exptl}$. For coupling constants replace δ with J.

in which the theoretical and experimental chemical shifts differ by more than 8 ppm (for C-3 the residue is 10.8 ppm, for C-19 the residue is 12.2 ppm).
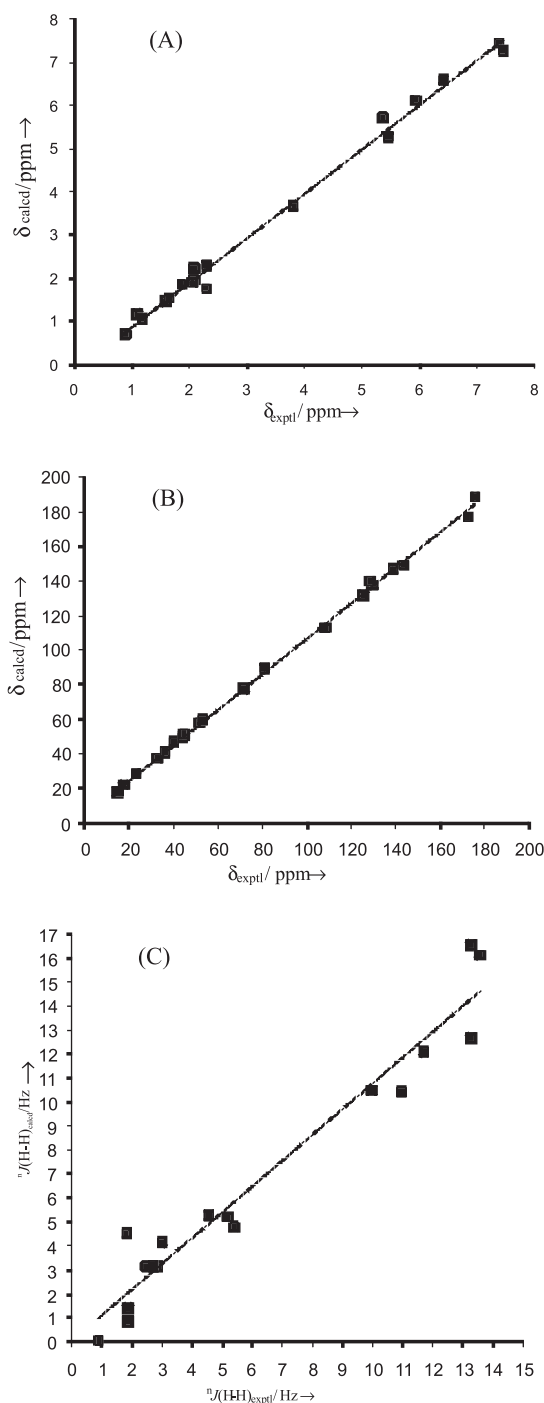

Figure 4. Correlation between calculated (B3PW91/DGDZVP) and experimental ^{1}H (A) ^{13}C (B) NMR chemical shifts and coupling constant [^nJ(H–H)] (C) of **2**.

Recently, we successfully used three-dimensional MEP surfaces to define the most probable sites of protonation of dipyridamole and on the study of the molecular mechanisms

the Diels-Alder reaction.[20] The MEP surfaces of **1** and **2** (Figure 5) in terms of total electron density show that the lowest electronic potential is in the proximity of oxygen atoms of the lactone (O1, O2), the hydroxyl group (O6) and the carbonyl group of ester (O5). The large negative potential of oxygen atoms may be regarded as a nucleophilic suction pump,[21] acting as a possible magnet for electrophilic attack of H^{+} or part of a biological receptor. The surfaces of **1** and **2** are visually similar, suggesting that **2** may have anti-ulcer activity similar to that of **1**. Experimental studies are being conducted to prove this hypothesis for **2**.
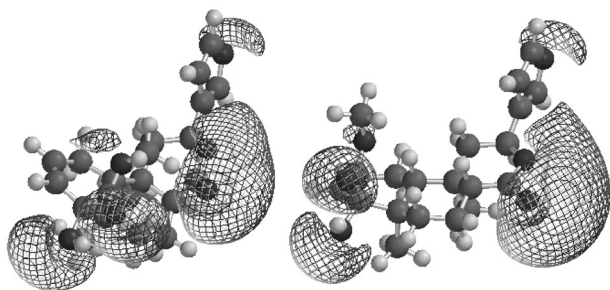

Figure 5. Three-dimensional MEP surfaces for **1** (A) and **2** (B).

Experimental

General Experimental Procedures

IR spectra were recorded on NaCl for compound **3** and using the pure substance for compound **2**. ^{1}H and ^{13}C NMR data were obtained at 300 and 75.4 MHz, respectively, in CDCl$_3$ using the solvent peak as the internal standard. EIMS spectra were obtained at 70 eV (probe) for compound **3** and HREI-MS data were obtained for compound **2**. TLC was on silica gel 60H (Merck 7736) and CC on silica gel (Merck 7734).

Plant Material

Croton palanostigma Klotzsch (Euphorbiaceae) was collected in March 2007 in Terra Alta, Pará, Brazil. A voucher specimen was identified by Dr. Ricardo Secco and is deposited in the herbarium of Museu Paraense Emílio Goeldi, Belém, Pará, Brazil (MG 182.822).

Extraction and isolation

Dried and powdered bark (740 g) and leaves (590 g) of *C. palanostigma* were successively extracted in a Soxhlet apparatus using hexane, CH$_2$Cl$_2$ and MeOH. During concentration of the hexane bark extract, a white solid (1.5 g) composed mainly of aparisthman and cordatin

(**1**) (1:1) precipitated. The remaining hexane bark extract was concentrated under vacuum to yield a gum (20.5 g). The gum was subjected to CC and TLC on silica gel and eluted with mixtures of hexane, EtOAc and MeOH in increasing order of polarity, yielding aparisthman[2] (800 mg), **1**[3] (60 mg), **3**[14] (7 mg), *ent*-trachyloban-18-oic acid[22] (217 mg), *ent*-13-epimanoyl oxide[19] (40 mg), *ent*-3-oxo-13-epimanoyl oxide[19] (18 mg) *ent*-3β-hydroxy-13-epimanoyl oxide[19] + 3-*O*-acetylaleuritolic acid[23] (6 mg), sitosterol[24,25] + stigmasterol[25] (13 mg), stigmastan-3-one[26] (5 mg), 6β-hydroxystigmast-4-en-3-one[27] + 6β-hydroxystigmasta-4,22-dien-3-one[28] (41 mg), stigmast-4-en-3-one[27] + stigmasta-4,22-dien-3-one[29] (13 mg) and 3-*O*-acetylaleuritolic acid[23] (127 mg). The dichloromethane bark extract was concentrated under vacuum to yield a gum (5.1 g). The gum was subjected to CC and TLC and eluted with mixtures of hexane, EtOAc and MeOH in increasing order of polarity, yielding **1**[3] (270 mg) and the new compound 8-epicordatin (**2**) (20 mg). The hexane leaf extract was concentrated under vacuum to yield a gum (2.6 g). The gum was subjected to CC and TLC and eluted with hexane, EtOAc and MeOH in increasing order of polarity, yielding α-amyrenone[30] + 24-methylenecycloartenone[31] + lupenone[30,32] (31 mg) and 11α-hydroxyurs-12-en-3-one[33] (10 mg).

Crystallography

A single crystal of **2** was mounted on glass fiber in random orientation. Data collection was performed at room temperature using a Siemens Smart CCD diffractometer with graphite-monochromated Mo-K$_\alpha$ radiation (λ = 0.71073 A) with a nominal crystal detection distance of 4.0 cm. A hemisphere of data was collected based on three ω-scans (starting ω = –28°) at values of ϕ = 0°, 90° and 180° with the detector at 2θ = 28°. For each of these runs, frames (606, 435 and 230, respectively) were collected at 0.3° intervals using 30 s *per* frame.

The diffraction frames were integrated using the SAINT package[34] and corrected for absorption using SADABS.[35]

Table 2 shows a summary of data collection and refinement conditions for the crystal structure.

Computational Methods

Since it was difficult to define chemical shifts for hydrogens H-7α and H-7β, theoretical NMR calculations at the B3PW91/DGDZVP level were used to confirm the assignments. Similar methods involving comparison of experimental and theoretical NMR data have been reported for aparisthman,[36] strychnine,[37] corianlactone,[37]

daphnipaxinin,[37] boletunone B,[37] julocrotine,[38] cordatin[1] and others.

The geometry obtained from X-ray diffraction data of **2** was used as input for the full geometry optimization. This molecular conformation was optimized using the B3LYP hybrid functional,[39] together with the 6-31G(d,p) basis in the Gaussian 03 molecular package.[40] Vibrational analysis was carried out for the complete equilibrium geometry obtained by the procedure in the Gaussian 03 package at the DFT level with the B3LYP/6-31G(d,p) level in the gas phase, ensuring that each gradient optimization located was indeed a true minimum energy structure (no imaginary frequencies). Normal modes were analyzed visually using Hyperchem 7.5.[41] NMR (^{1}H and ^{13}C chemical shifts and coupling constants) spectra were calculated by the B3PW91/DGDZVP method in the gas phase for the geometry optimized using the B3LYP/6-31G(d,p) method. The use of a method for geometry optimization (B3LYP/6-31G(d,p)) and another one for NMR calculation has been successfully used by Bagno *et al.* (2006)[37] to predict NMR data of several natural products. Recently, we have successfully used this methodology to study ^{1}H and ^{13}C NMR spectra of cordatin.[1] In this case the geometry obtained was similar to that observed by X-Ray diffraction and could be used in calculations of NMR proprieties. All calculations were performed using Gaussian 03.[40] Linear regression analysis of NMR data was performed and relevant parameters were selected: correlation coefficients (R^2), Fisher ratio values (F), the standard deviation (s) and the predictive ability of the model (Q^2). MINITAB® release 14 was used for statistical analysis.[42]

The MEP surface was generated using HF/6-31G(d,p) with the geometry optimized in B3LYP/6-31G(d,p) and an isopotential of –20.0 a.u. On the MEP surface, regions indicating excess negative potential correspond to excess negative charges, i.e., attraction of the positively charged probe. The MEP surface was calculated and analyzed visually using the PC Spartan PRO molecular package.[43]

*8-Epicordatin (**2**)*

Crystals; Dec. 174-176 °C; $[\alpha]_D^{25}$ +107.35° (*c* 0.19, CHCl$_3$); IR ν_{max}/cm^{-1}: 3540, 3100, 2947, 1733, 1704, 1503, 1429, 1367, 1246, 1132, 1089, 873; ^{1}H NMR: see Table 1 and ^{13}C NMR: see Table 1; HRMS *m/z* [M+Na]$^+$ 397.1635 (calc. for C$_{21}$H$_{26}$O$_6$+Na, 397.1627); X-ray crystallography data: see Table 3 and Figure 3.

*12-Oxohardwickiic acid methyl ester (**3**)*

Oil. $[\alpha]_D^{25}$ –24.07° (*c* 0.054, CHCl$_3$); IR ν_{max}/cm^{-1}: 3135, 1714, 1668, 1509, 1461, 1250, 1232, 1157, 872; ^{1}H NMR: see Table 1 and ^{13}C NMR: see Table 1; EIMS *m/z* (rel. int.):

344 [M]$^+$ (0.3), 313 [M–OMe]$^+$ (2.6), 284 [M–HCO$_2$Me]$^+$ (0.5), 236 (10.0), 235 (57.3), 234 [M–CH$_2$=C-furyl]$^+$ (19.8), 233 (5.3), 220 (21.2), 219 [234–Me]$^+$ (100), 218 (13.7), 217 (7.0), 187 (15.7), 175 (3.1), 105 (4.0), 95 (10.5).

Conclusions

The chemical study of the bark and leaves of *Croton palanostigma* Klotzsch (Euphorbiaceae) led to the isolation of a new clerodane diterpene, 8-epicordatin. X-ray diffraction, NMR experiments and theoretical calculations were used to propose the structure of this compound. The calculated geometric parameters are close to the X-ray crystal structure indicating the accuracy of theoretical method used. The NMR theoretical values show good correlation and high predictive power and could be used to confirm the chemical shifts of hydrogens H-7α and H-7β. Therefore, DFT calculations can attain a considerable degree of accuracy in the prediction of the ^{13}C and ^{1}H NMR spectra of complex organic molecules such as natural products. The MEP surfaces of cordatin and 8-epicordatin shows four sites susceptible of protonation (O1, O2, O5 and O6 positions) indicating that these species might, consequently, interact with the extracellular surface of the H$^+$, K$^+$-ATPase.

Supplementary Information

Crystallographic data for the structure reported in this paper have been deposited with the Cambridge Crystallographic Data Centre, number CCDC 666036. Copies of the data can be obtained, free of charge, on application to the Director, CCDC, 12 Union Road, Cambridge CB2 1EZ, UK (fax: +44-1223-336033 or e-mail: deposit@ccdc.cam.ac.uk).

Acknowledgments

References

1. Brasil, D. S. B.; Alves, C. N.; Guilhon, G. M. S. P.; Müller, A. H.; Secco, R. de S.; Peris, G.; Llusar, R.; *Int. J. Quantum Chem.* **2008**, *108*, 2564; Brasil, D. S. B.; Müller, A. H.; Guilhon, G. M. S. P.; Alves, C. N.; Andrade, E. H. A.; da Silva, J. K. R.; Maia, J. G. S.; *J. Braz. Chem. Soc.* **2009**, *20*, 1188.

2. Müller, A. H.; Oster, B.; Schukmann, W. K.; Bartl, H.; *Phytochemistry* **1986**, *25*, 1415.

3. Dadoun, H.; Müller, A. H.; Cesario, M.; Guilhem, J.; Pascard, C.; *Phytochemistry* **1987**, *26*, 2108.

4. Hiruma-Lima, C. A.; Gracioso, J. S.; Toma, W.; Almeida, A. B.; Paula, A. C. B.; Brasil, D. S. B.; Müller, A. H.; Souza Brito, A. R. M.; *Phytomedicine* **2001**, *8*, 94.

5. Hiruma-Lima, C. A.; Gracioso, J. S.; Toma, W.; Paula, A. C. B; Almeida, A. B. A.; Brasil, D. S. B.; Müller, A. H.; Souza Brito, A. R. M.; *Biol. Pharm. Bull.* **2000**, *23*, 1465.

6. Salatino, A.; Salatino, M. L. F.; Negri, G.; *J. Braz. Chem. Soc.* **2007**, *18*, 11; Sandoval, M.; Ayala, S.; Oré, M.; Valdivieso, L.; Loli, R.; Ricra, V; Huaman, O.; *An. Fac. Med. Lima* **2005**, *66*, 119; Sandoval, M.; Ayala, S.; Oré, R.; Arroyo, J.; *An. Fac. Med. Lima* **2002**, *63*, 251; Ayala, S.; Jurupe, H.; Díaz, D.; Lock, O.; Vega, M.; Luque, J.; Garnique, M.; *An. Fac. Med. Lima* **2001**, *62*, 317; Ayala, S.; Díaz, D.; Palomino, M.; Armas, S.; Paz, J.; *An. Fac. Med. Lima* **1999**, *60*, 22; Ayala, S.; Jurupe, H.; Díaz, D.; Oré, R.; Cárdenas, W.; Espejo, L.; *Rev. Situa* **2000**, *8*, 12; Sandoval, M.; Ayala, S.; Oré, R.; Loli, A.; Huaman, O.; Valdivieso, R.; Béjar, E.; *An. Fac. Med. Lima* **2006**, *67*, 199; Sandoval, M.; Okuhama, N. N.; Clark, M.; Angeles, F. M.; Lao, J.; Bustamante, S.; Miller, M. J. S.; *J. Ethnopharmacol.* **2002**, *80*, 121.

7. Perdue, G. P.; Blomster, R. N.; Blake, D. A.; Farnsworth, N. R.; *J. Pharm. Sci.* **1979**, *68*,124.

8. Pieters, L. A. C.; Vanden Berghe, D. A.; Vlietinck, A. J.; *Phytochemistry* **1990**, *29*, 348.

9. Pieters, L.; De Bruyne, T.; Claeys, M.; Vlietinck, A.; Calomme, M.; Vanden Berghe, D.; *J. Nat. Prod.* **1993**, *56*, 899.

10. Cai, Y.; Evans, F. J.; Roberts, M. F.; Phillipson, J. D.; Zenk, M. H.; Gleba, Y. Y.; *Phytochemistry* **1991**, *30*, 2033.

11. Lorentzon, P.; Bayati, A.; Lee, H.; Andersen, K.; *Ann. NY Acad. Sci.* **1997**, *834*, 592.

12. Sachs, G.; Shin, J. M.; Briving, C.; Wallmark, B.; Hersey, S.; *Annu. Rev. Pharmacol. Toxicol.* **1995**, *35*, 277.

13. Kubota, T.; *Tetrahedron* **1958**, *4*, 68.

14. McChesney, J. D.; Silveira, E. R.; *Phytochemistry* **1989**, *28*, 3411.

15. De Araujo-Junior, V. T.; Navarro, P. A.; Silva, M. S.; Da-Cunha, E. V. L.; De Fatima Agra, M.; Gray, A. I.; Barbosa-Filho, J. M.; *Ciencia (Maracaibo, Venezuela)* **2002**, *10*, 286.

16. Palmeira-Junior, S. F.; Conserva, L. M.; Silveira, E. R.; *J. Braz. Chem. Soc.* **2005**, *16*, 1420.

17. Mambu, L.; Ramanandraibe, V.; Martin, M. T.; Blond, A.; Grellier, P.; Frappier, F.; *Planta Med.* **2002**, *68*, 377.

18. Faulkner, D. F.; Lebby, V.; Waterman, P. G.; *Planta Med.* **1985**, *51*, 354.

19. Konishi, T.; Azuma, M.; Itoga, R.; Kiyosawa, S.; Fujiwara, Y.; Shimada, Y.; *Chem. Pharm. Bull.* **1996**, *44*, 229.

20. Alves, C. N.; Da Silva, A. B. F.; Castilho, M.; Mazo, L. H.; Tabak, M.; *Chem. Phys. Lett.* **2001**, *349*, 146; Domingo, L. R.; Andres, J.; Alves, C. N.; *Eur. J. Org. Chem.* **2002**, *15*, 2557.

21. Lamotte-Brasseur, J.; Dive, G.; Dehareng, D.; Ghuysen, J. M.; *J. Theor. Biol.* **1990**, *145*, 183.

22. Leong, Y.-W.; Harrison, L. J.; *Phytochemistry* **1997**, *45*, 1457.

23. Addae-Mensah, I.; Achenbach, H.; Thoithi, G. N.; Waibel, R.; Mwangi, J. W.; *Phytochemistry* **1992**, *31*, 2055.

24. Nes, W. D.; Norton, R. A.; Benson, M.; *Phytochemistry* **1992**, *31*, 805.

25. De-Eknamkul, W.; Potduang, B.; *Phytochemistry* **2003**, *62*, 389.

26. Zhao, Y-X.; Li, C-S.; Luo, X-D.; Yi, T-M.; Zhou, J.; *Chin. J. Org. Chem.* **2005**, *25*, 1100.

27. Greca, M. D.; Monaco, P.; Previtera, L.; *J. Nat. Prod.* **1990**, *53*, 1430.

28. Asha, K. N.; Chowdhury, R.; Hasan, C. M.; Rashid, M. A.; *Acta Pharm.* **2004**, *54*, 57.

29. Almeida, M. L. S.; Kocovský, P.; Bäckvall, J-E.; *J. Org. Chem.* **1996**, *61*, 6587; Shu, Y.; Jones, S. R.; Kinney, W. A.; Selinsky, B. S.; *Steroids* **2002**, *67*, 291.

30. Olea, R. S. G.; Roque, N. F.; *Quim. Nova* **1990**, *13*, 278.

31. Barla, A.; Birman, H.; Kultur, S.; Oksuz, S.; *Turk. J. Chem.* **2006**, *30*, 325; Jayasinghe, U. L. B.; Vithana, H. S. K.; Wannigama, G. P.; Fujimoto, Y.; *Fitoterapia* **2001**, *72*, 594.

32. Ahmad, V. U.; Rahman, A. U.; Pentacyclic Triterpenoids, *Handbook of Natural Products Data*, Elsevier: Amsterdam, vol. 2, 1994.

33. Hou, Z-F.; Xie, Z-X.; Tu, Y-Q.; Li, Y.; *Indian J. Chem., Sect. B: Org. Chem. Incl. Med. Chem.* **2002**, *41*, 234.

34. SAINT version 6.26 A. Bruker Analytical X-ray Systems: Madison, WI.

35. Sheldrick, G. M. SADABS empirical absorption program, V 2.03, University of Gottingen, 1996.

36. Brasil, D. S. B.; Moreira, R. Y. O.; Müller, A. H.; Alves, C. N.; *Int. J. Quantum Chem.* **2006**, *106*, 2706.

37. Bagno, A.; Rastrelli, F.; Saielli, G.; *Chem.-A Eur. J.* **2006**, *12*, 5514.

38. Moreira, R. Y. O.; Brasil, D. S. B.; Alves, C. N.; Guilhon, G. M. S. P.; Santos, L. S.; Arruda, M. S. P.; Müller, A. H.; Barbosa, P. S.; Abreu, A. S.; Silva, E. O.; Rumjanek, V. M.; Souza, J. Jr.; Silva, A. B. F.; Santos, R. H. A.; *Int. J. Quantum Chem.* **2008**, *108*, 513.

39. Becke, A. D.; *J. Chem. Phys.* **1993**, *98*, 5648; Lee, C.; Yang, W.; Parr, R. G.; *Phys. Rev. B* **1988**, *37*, 785.

40. Frisch, M. J.; Trucks, G. W.; Schlegel, H. B.; Scuseria, G. E.; Robb, M. A.; Cheeseman, J. R.; Montgomery, J. A., Jr.; Vreven,

T.; Kudin, K. N.; Burant, J. C.; Millam, J. M.; Iyengar, S. S.; Tomasi, J.; Barone, V.; Mennucci, B.; Cossi, M.; Scalmani, G.; Rega, N.; Petersson, G. A.; Nakatsuji, H.; Hada, M.; Ehara, M.; Toyota, K.; Fukuda, R.; Hasegawa, J.; Ishida, M.; Nakajima, T.; Honda, Y.; Kitao, O.; Nakai, H.; Klene, M.; Li, X.; Knox, J. E.; Hratchian, H. P.; Cross, J. B.; Adamo, C.; Jaramillo, J.; Gomperts, R.; Stratmann, R. E.; Yazyev, O.; Austin, A. J.; Cammi, R.; Pomelli, C.; Ochterski, J. W.; Ayala, P. Y.; Morokuma, K.; Voth, G. A.; Salvador, P.; Dannenberg, J. J.; Zakrzewski, V. G.; Dapprich, S.; Daniels, A. D.; Strain, M. C.; Farkas, O.; Malick, D. K.; Rabuck, A. D.; Raghavachari, K.; Foresman, J. B.; Ortiz, J. V.; Cui, Q.; Baboul, A. G.; Clifford, S.; Cioslowski, J.; Stefanov, B. B.; Liu, G.; Liashenko, A.; Piskorz, P.; Komaromi, I.; Martin, R. L.; Fox, D. J.; Keith, T.; Al-Laham, M. A.; Peng, C. Y.; Nanayakkara, A.; Challacombe, M.; Gill, P. M. W.; Johnson, B.; Chen, W.; Wong, M. W.; Gonzalez, C.; Pople, J. A.; Gaussian 03, Revision B.04. Gaussian: Pittsburgh, PA, 2003.

41. HyperChem™ Release 7.5 for Windows Molecular Modeling System. Hypercube: Gainesville, USA, 2002.

42. MINITAB Release 14 for Windows. Minitab: State College, PA, 2003.

43. *PC Spartan-Pro*, version 1.0; Wavefunction, Inc.: Irvine, CA, USA, 1999.

Isolation, X-ray Crystal Structure and Theoretical Calculations of the New Compound 8-epicordatin and Identification of Others Terpenes and Steroids from the Bark and Leaves of *Croton palanostigma* Klotzsch

Davi S. B. Brasil,[a,b] Adolfo H. Müller,*,[a,c] Gisele M. S. P. Guilhon,[a] Cláudio N. Alves,[a] Gabriel Peris,[d] Rosa Llusar[d] and Vicent Moliner[d]

[a]*Instituto de Ciências Exatas e Naturais, Universidade Federal do Pará, Av. Augusto Corrêa, 01, 66075-900 Belém-PA, Brazil*

[b]*Faculdade de Engenharia Química, Instituto de Tecnologia, Universidade Federal do Pará, Av. Augusto Corrêa, 01, 66075-900 Belém-PA, Brazil*

[c]*Centro Universitário do Estado do Pará, Av Nazaré, 630, 66035-170 Belém-PA, Brazil*

[d]*Departament de Química Física i Analítica, Universitat Jaume I, 12071, Castellón, Spain*

Table S1. Atomic coordinates (x 10^4) and equivalent isotropic displacement parameters (Å^{2}x 10^3) for **2** U(eq) is defined as one third of the trace of the orthogonalized U^{ij} tensor

	x	y	z	U(eq)
O(4)	2238(2)	4025(2)	774(1)	57(1)
O(5)	2280(2)	5725(2)	438(1)	73(1)
C(2)	2821(3)	4243(3)	2029(1)	53(1)
C(19)	2505(2)	5093(2)	781(1)	49(1)
C(9)	5490(2)	3141(3)	1335(1)	52(1)
O(6)	3060(3)	6646(2)	1274(1)	80(1)
C(1)	3861(2)	3587(2)	1948(1)	49(1)
C(5)	4368(2)	5055(3)	1284(1)	49(1)
O(1)	7063(2)	1733(4)	825(1)	96(1)
C(10)	4370(2)	3781(2)	1419(1)	42(1)
C(8)	5963(2)	3455(3)	806(1)	63(1)
C(11)	5223(2)	1897(3)	1284(1)	60(1)
C(3)	2486(3)	5056(3)	1727(1)	56(1)
C(4)	3117(3)	5450(2)	1269(1)	51(1)

	x	y	z	U(eq)
C(13)	5926(3)	123(4)	880(1)	73(1)
C(7)	6060(3)	4715(4)	720(1)	77(1)
C(20)	6359(3)	3319(4)	1759(1)	73(1)
O(2)	7815(2)	3222(4)	483(1)	119(1)
C(18)	4970(3)	5775(3)	1692(1)	72(1)
C(14)	5757(4)	−36(4)	359(2)	92(1)
C(17)	7009(3)	2817(6)	695(1)	90(2)
O(10)	5358(4)	−1610(3)	747(2)	130(1)
C(6)	4921(3)	5245(3)	762(1)	66(1)
C(12)	6241(3)	1182(4)	1146(1)	78(1)
C(15)	5419(5)	−1082(4)	295(2)	104(2)
C(16)	5672(5)	−853(6)	1105(2)	111(2)
C(21)	1641(3)	3616(3)	336(1)	68(1)

*e-mail: muller@ufpa.br, muller@cesupa.br

Table S2. Bond lengths [Å] and angles [°] for **2**

O(4)-C(19)	1.317(4)	C(20)-C(9)-C(10)	114.2(2)
O(4)-C(21)	1.437(3)	C(8)-C(9)-C(10)	108.9(2)
O(5)-C(19)	1.205(3)	C(2)-C(1)-C(10)	112.4(2)
C(2)-C(3)	1.315(4)	C(6)-C(5)-C(18)	109.3(2)
C(2)-C(1)	1.486(4)	C(6)-C(5)-C(10)	110.2(3)
C(19)-C(4)	1.533(4)	C(18)-C(5)-C(10)	112.6(2)
C(9)-C(11)	1.528(5)	C(6)-C(5)-C(4)	110.1(2)
C(9)-C(20)	1.536(4)	C(18)-C(5)-C(4)	107.1(3)
C(9)-C(8)	1.541(4)	C(10)-C(5)-C(4)	107.5(2)
C(9)-C(10)	1.558(4)	C(17)-O(1)-C(12)	123.5(3)
O(6)-C(4)	1.432(4)	C(1)-C(10)-C(9)	113.3(2)
C(1)-C(10)	1.530(3)	C(1)-C(10)-C(5)	110.6(2)
C(5)-C(6)	1.535(4)	C(9)-C(10)-C(5)	116.6(2)
C(5)-C(18)	1.549(4)	C(17)-C(8)-C(7)	114.3(3)
C(5)-C(10)	1.565(4)	C(17)-C(8)-C(9)	111.0(3)
C(5)-C(4)	1.570(4)	C(7)-C(8)-C(9)	113.6(3)
O(1)-C(17)	1.344(6)	C(9)-C(11)-C(12)	113.4(3)
O(1)-C(12)	1.451(5)	C(2)-C(3)-C(4)	124.1(3)
C(8)-C(17)	1.493(6)	O(6)-C(4)-C(3)	106.5(3)
C(8)-C(7)	1.529(6)	O(6)-C(4)-C(19)	105.3(2)
C(11)-C(12)	1.531(5)	C(3)-C(4)-C(19)	109.9(2)
C(3)-C(4)	1.494(4)	O(6)-C(4)-C(5)	110.2(2)
C(13)-C(16)	1.342(7)	C(3)-C(4)-C(5)	111.5(2)
C(13)-C(14)	1.393(6)	C(19)-C(4)-C(5)	113.1(2)
C(13)-C(12)	1.494(6)	C(16)-C(13)-C(14)	106.1(5)
C(7)-C(6)	1.507(6)	C(16)-C(13)-C(12)	126.3(4)
O(2)-C(17)	1.214(5)	C(14)-C(13)-C(12)	127.5(4)
C(14)-C(15)	1.326(7)	C(6)-C(7)-C(8)	109.6(3)
O(10)-C(15)	1.342(7)	C(15)-C(14)-C(13)	107.3(4)
O(10)-C(16)	1.356(7)	O(2)-C(17)-O(1)	117.6(4)
C(19)-O(4)-C(21)	117.5(2)	O(2)-C(17)-C(8)	123.5(6)
C(3)-C(2)-C(1)	124.1(3)	O(1)-C(17)-C(8)	118.9(4)
O(5)-C(19)-O(4)	123.0(3)	C(15)-O(10)-C(16)	106.3(4)
O(5)-C(19)-C(4)	123.6(3)	C(7)-C(6)-C(5)	113.1(3)
O(4)-C(19)-C(4)	113.4(2)	O(1)-C(12)-C(13)	106.6(3)
C(11)-C(9)-C(20)	109.8(3)	O(1)-C(12)-C(11)	115.0(4)
C(11)-C(9)-C(8)	103.6(2)	C(13)-C(12)-C(11)	112.5(3)
C(20)-C(9)-C(8)	111.5(2)	C(14)-C(15)-O(10)	110.4(5)
C(11)-C(9)-C(10)	108.1(2)	C(13)-C(16)-O(10)	109.9(4)

Symmetry transformations used to generate equivalent atoms

Table S3. Anisotropic displacement parameters (Å^2x 10^3) for **2**. The anisotropic displacement factor exponent takes the form: $-2\pi^2[h^2\, a^{*2}U^{11} + \dots + 2\, h\, k\, a^*\, b^*\, U^{12}\,]$

	U^{11}	U^{22}	U^{33}	U^{23}	U^{13}	U^{12}
O(4)	69(1)	50(1)	53(1)	3(1)	−18(1)	−9(1)
O(5)	95(2)	63(1)	61(1)	13(1)	−22(1)	−3(1)
C(2)	60(2)	60(2)	37(1)	−7(1)	13(1)	3(1)
C(19)	54(2)	51(2)	43(1)	3(1)	1(1)	−1(1)
C(9)	33(1)	88(2)	35(1)	−9(1)	−1(1)	−5(1)
O(6)	123(2)	44(1)	73(1)	−6(1)	−14(2)	−7(1)
C(1)	49(2)	57(2)	40(1)	3(1)	8(1)	0(1)
C(5)	53(2)	59(2)	35(1)	−1(1)	−1(1)	−20(1)
O(1)	41(1)	150(3)	96(2)	−35(2)	12(1)	15(2)
C(10)	35(1)	59(2)	32(1)	−3(1)	1(1)	-6(1)
C(8)	39(2)	114(3)	36(1)	−12(2)	3(1)	−19(2)
C(11)	39(2)	87(2)	53(2)	−9(2)	0(1)	13(2)
C(3)	62(2)	64(2)	41(1)	−8(1)	5(1)	10(2)
C(4)	67(2)	42(2)	45(1)	−3(1)	−4(1)	−6(1)
C(13)	62(2)	97(3)	58(2)	11(2)	5(2)	47(2)
C(7)	59(2)	128(3)	44(2)	3(2)	8(2)	−39(2)
C(20)	42(2)	134(3)	44(2)	−10(2)	−7(1)	−7(2)
O(2)	55(2)	211(4)	92(2)	−36(2)	37(2)	−28(2)
C(18)	89(3)	78(2)	48(2)	−8(2)	−5(2)	−39(2)
C(14)	118(4)	82(3)	77(3)	8(2)	0(2)	32(3)
C(17)	47(2)	173(5)	52(2)	−38(3)	11(2)	−4(3)
O(10)	149(3)	99(3)	142(3)	26(3)	40(3)	40(2)
C(6)	69(2)	82(2)	46(2)	7(2)	4(2)	−33(2)
C(12)	49(2)	129(4)	57(2)	−8(2)	−4(2)	34(2)
C(15)	133(4)	69(3)	111(4)	−17(3)	−10(3)	28(3)
C(16)	118(4)	125(4)	89(3)	27(3)	33(3)	52(3)
C(21)	73(2)	68(2)	62(2)	−4(2)	−24(2)	−11(2)

Table S4.   Hydrogen coordinates (x 10^4) and isotropic displacement parameters (Å^2 x 10^3) for **2**

	x	y	z	U(eq)
H(2)	2379	4068	2310	63
H(6)	2917	6874	986	120
H(1A)	3696	2798	1989	59
H(1B)	4404	3792	2207	59
H(10)	3841	3439	1180	50
H(8)	5411	3191	557	75
H(11A)	4656	1800	1023	72
H(11B)	4914	1631	1604	72
H(3)	1813	5408	1804	67
H(7A)	6558	5037	973	92
H(7B)	6371	4859	384	92
H(20A)	6035	3130	2083	110
H(20B)	6590	4087	1762	110
H(20C)	6996	2850	1697	110
H(18A)	5725	5516	1732	108
H(18B)	4583	5712	2012	108
H(18C)	4976	6542	1584	108
H(14)	5861	494	103	111
H(6A)	4441	4940	497	79
H(6B)	4990	6042	702	79
H(12)	6613	977	1466	94
H(15)	5248	-1405	-19	125
H(16)	5705	-991	1454	133
H(21A)	941	4001	306	102
H(21B)	1507	2829	374	102
H(21C)	2078	3743	33	102

Table S5. Theoretical and Experimental NMR Chemical Shifts for **2**

Position	8-*epi*-cordatin (**2**) calculated[a]		8-*epi*-cordatin (**2**) experimental	
	δ_C	δ_H	δ_C	δ_H
1	28.0	1.95	22.9	2.1
2	137.6	6.14	130.0	5.95
3	139.5	5.71	128.7	5.36
4	88.8		81.2	
5	46.7		40.5	
6	37.0	α - 1.87 β - 0.71	33.2	α - 1.86 β - 0.91
7	22.5	α - 1.43 β - 2.22	18.1	α - 1.60 β - 2.10
8	57.7	1.90	51.4	2.07
9	40.7		36.4	
10	50.1	2.28	44.7	2.33
11	51.3	α - 1.79 β - 1.54	44.4	α - 2.29 β - 1.67
12	77.0	5.26	71.9	5.48
13	131.5		125.8	
14	113.2	6.57	108.5	6.41
15	149.5	7.45	143.7	7.41
16	146.4	7.26	139.3	7.44
17	177.1		171.9	
18	17.5	1.15	15.2	1.12
19	187.7		175.5	
20	18.7	1.04	15.4	1.17
21	59.4	3.66	53.2	3.81

[a] NMR chemical shifts calculated at B3PW91/DGDZVP.

Table S6. Predicted, calculated and Experimental ^{1}H NMR coupling constant [[n]*J*(H-H)] (Hz) for **2**

Coupling	experimental	B3PW91/ DGDZVP	Predicted[a]
2 - 1α	2.9	3.2	2.9
2 - 1β	4.6	5.3	4.8
2 - 3	10	10.5	9.7
3 - 1α	1.8	4.5	4.2
3 - 1β	2.5	3.2	2.9
6α - 6β	13.3	16.5	15.3
6α - 7α	2.7	3.2	2.9
6α - 7β	2.7	3.2	2.9
6β - 7α	13.3	12.7	11.7
6β - 7α	3.0	4.1	3.8
10 - 1α	11.0	10.4	9.6
10 - 1β	5.2	5.2	4.8
11α - 11β	13.6	16.2	15.0
11α - 12	5.4	4.8	4.4
12 - 11β	11.7	12.1	11.2
14 - 15	1.9	1.4	1.3
14 - 16	0.9	0.1	0.0
15 - 16	1.9	0.9	0.8

[a]Predicted after linear regression using the equation: $J_{calcd} = a + bJ_{exptl}$.
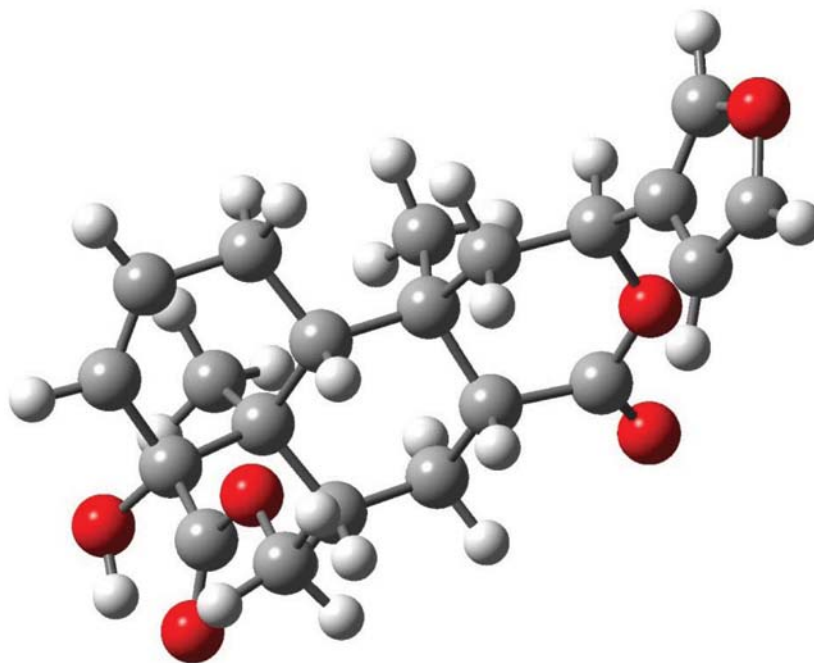
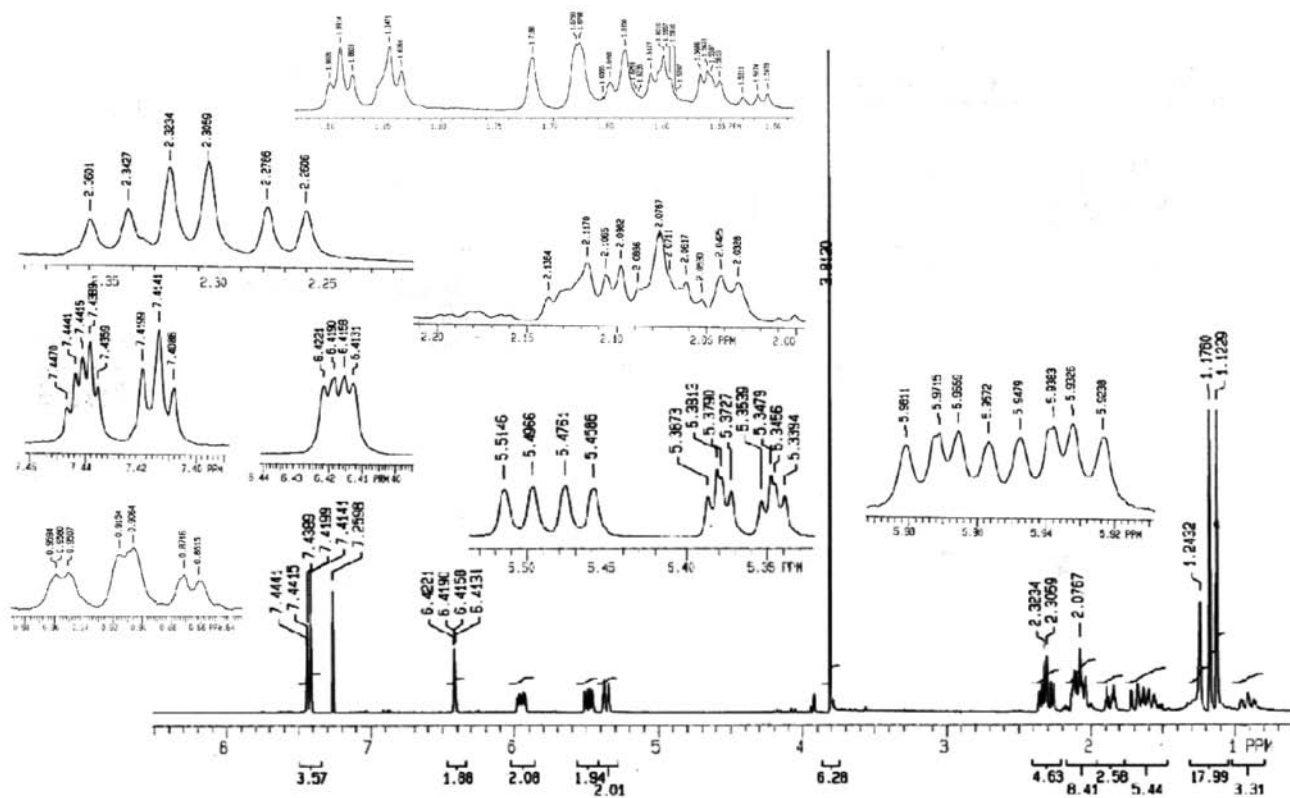**Figure S1**. B3LYP/6-31G(*d,p*) optimized structure of **2**.

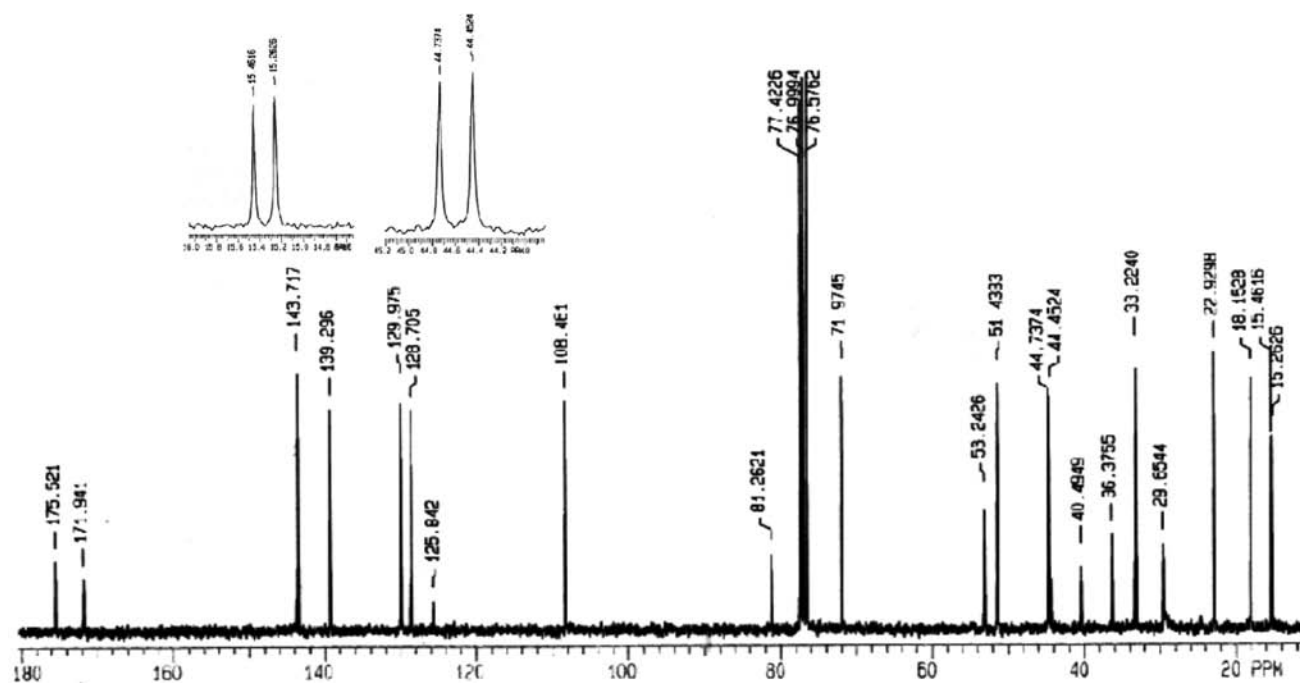**Figure S2**. ¹H NMR (300 MHz, CDCl₃) of the new compound **2**.

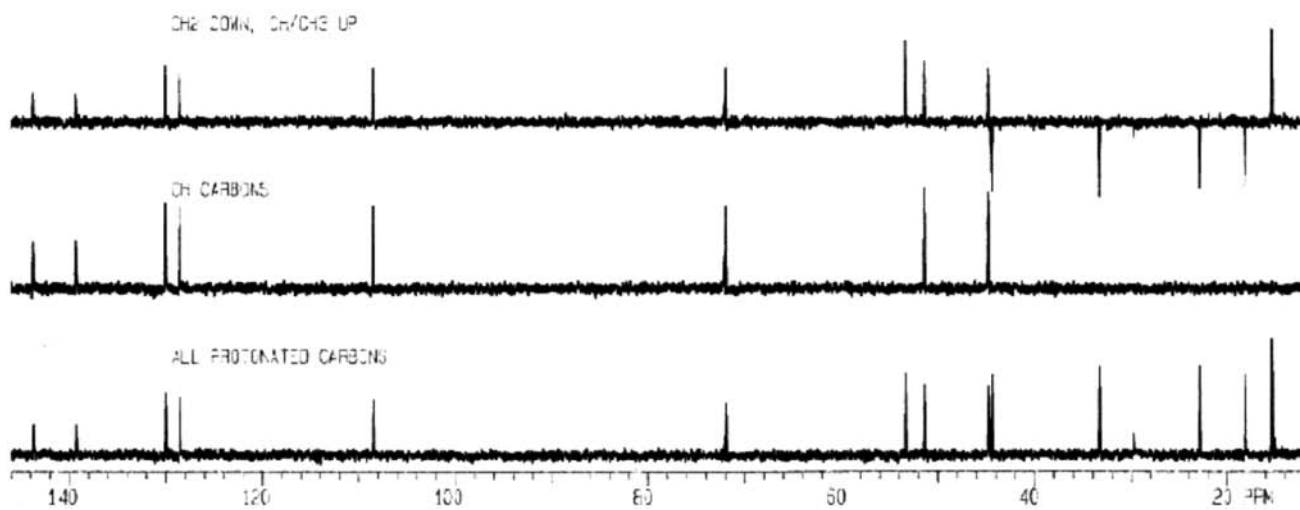**Figure S3**. ^{13}C NMR (75.4 MHz, CDCl$_3$) of the new compound **2**.
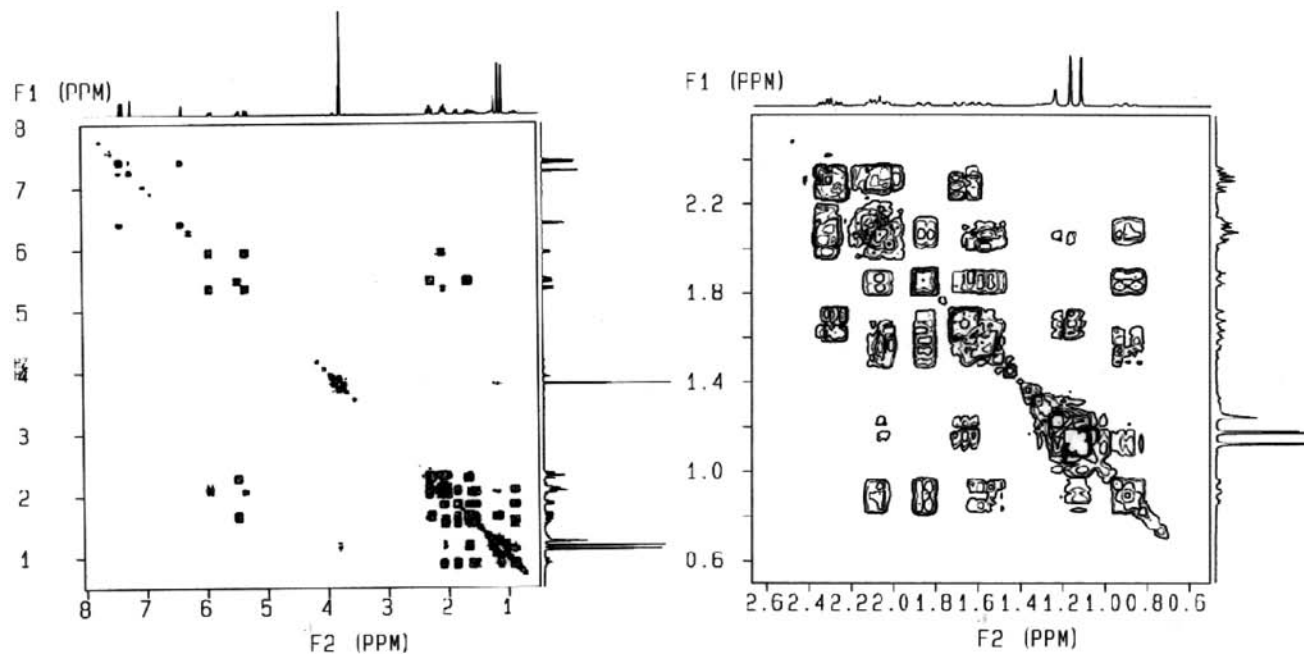
Figure S4. DEPT spectrum of the new compound **2**.
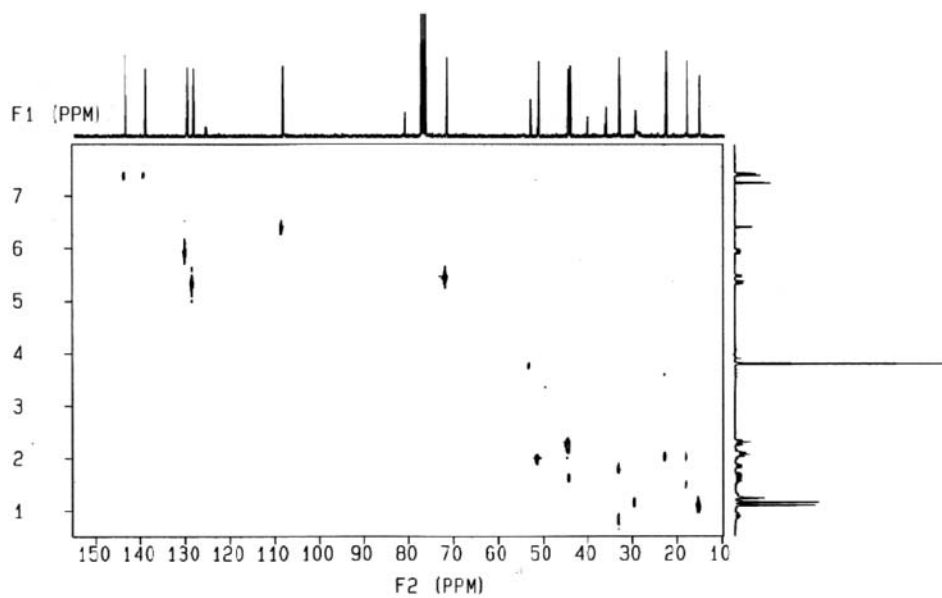
Figure S5. ¹H, ¹H- COSY spectrum of the new compound **2**.

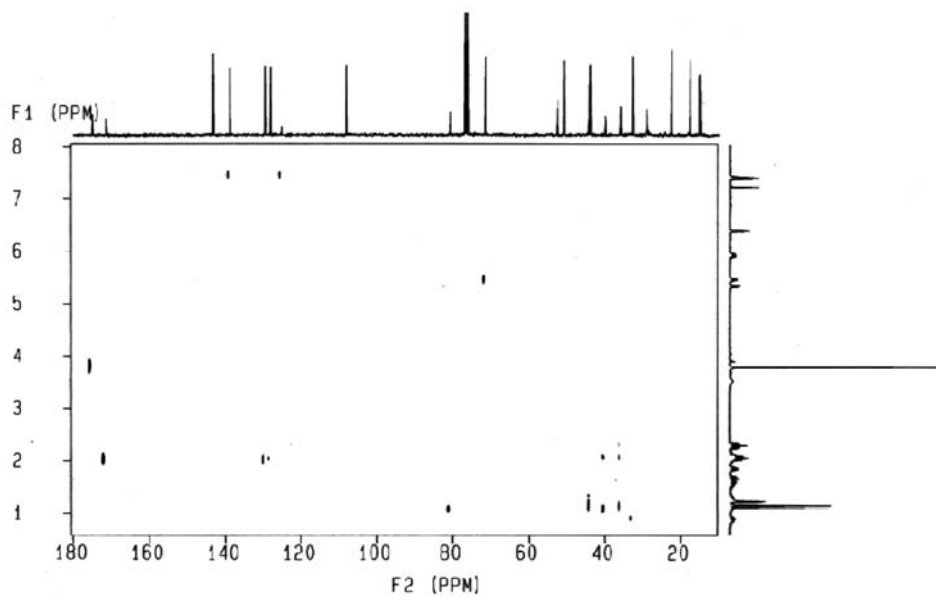**Figure S6**. HETCOR spectrum of the new compound **2**.

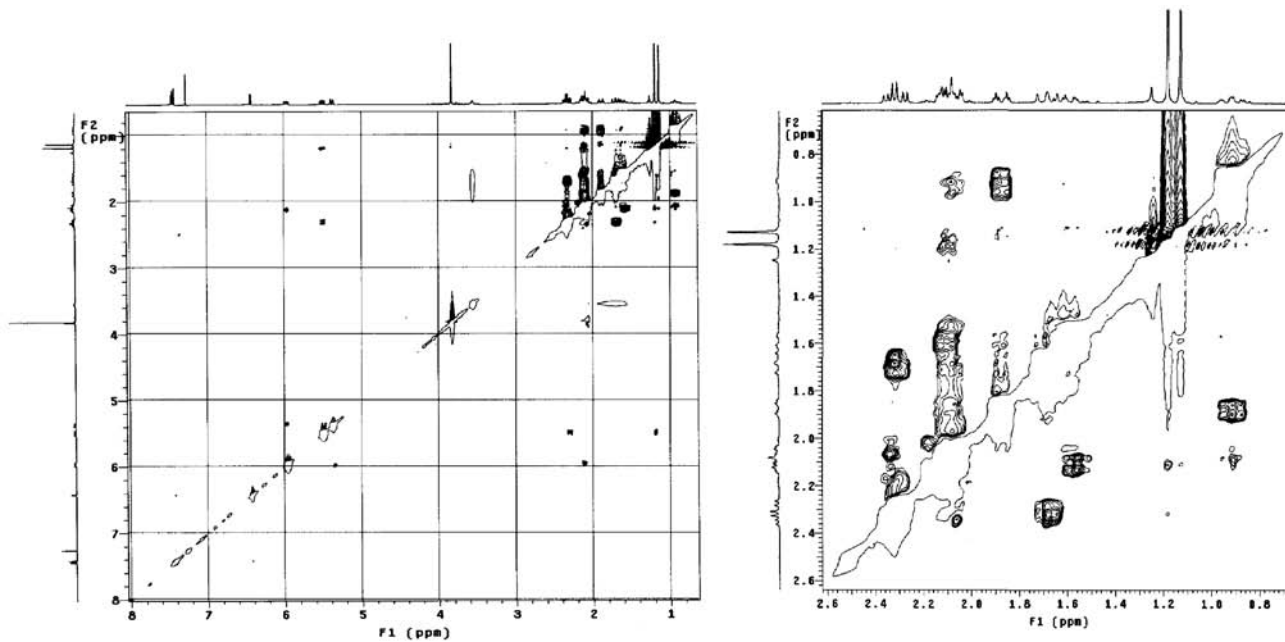**Figure S7**. COLOC spectrum of the new compound **2**.
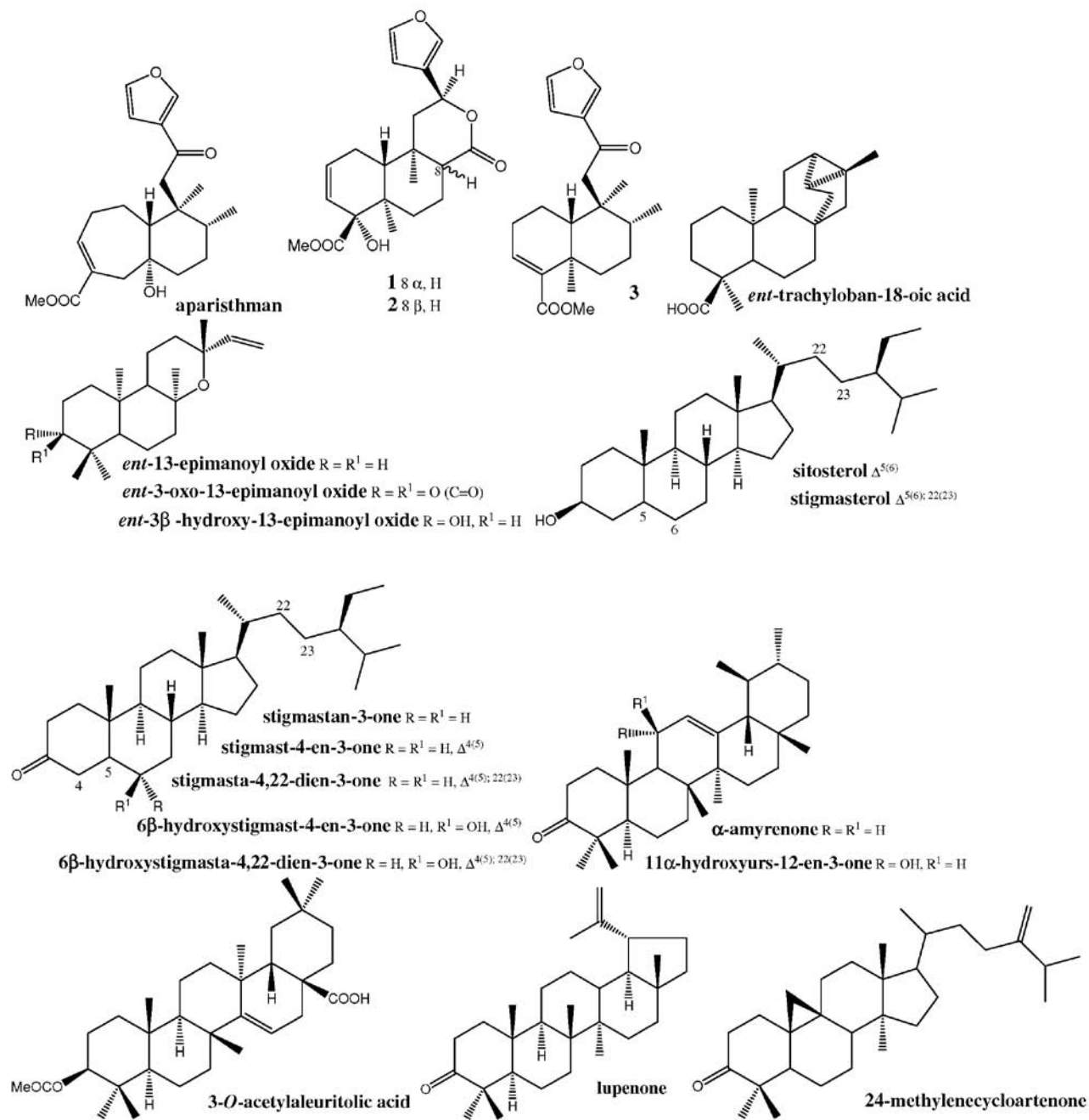

Figure S8. NOESY spectrum of the new compound **2**.

Figure S9. Structures of all identified compounds.